Available online at www.sciencedirect.com
ScienceDirect
Experimental Neurology 209 (2008) 181–191
Experimental Neurology
www.elsevier.com/locate/yexnr

MRI evidence of white matter damage in a mouse model of Nijmegen breakage syndrome

Yaniv Assaf [a,*], Ronit Galron [a], Itai Shapira [a], Anat Nitzan [a], Tamar Blumenfeld-Katzir [a], Arieh S. Solomon [b], Vered Holdengreber [c], Zhao-Qi Wang [d,e], Yosef Shiloh [f], Ari Barzilai [a]

[a] *Department of Neurobiochemistry, George S. Wise Faculty of Life Sciences, Tel Aviv University, Tel Aviv, 69978, Israel*
[b] *Goldschleger Eye Research Institute, Sheba Medical Center, Tel Hashomer 52621, Israel*
[c] *Department of Cell Research and Immunology, George S. Wise Faculty of Life Sciences, Tel Aviv University, Tel Aviv 69978, Israel*
[d] *Leibniz Institute for Age Research - Fritz Lipmann Institute e.V. D-07745, Jena, Germany*
[e] *Friedrich-Schiller-University of Jena, D-07745, Jena, Germany*
[f] *The David and Inez Myers Laboratory for Genetic Research, Department of Human Molecular Genetics and Biochemistry, Sackler School of Medicine, Tel Aviv University, Tel Aviv 69978, Israel*

Received 21 August 2007; accepted 14 September 2007
Available online 2 October 2007

Abstract

Nijmegen breakage syndrome (NBS) is a genomic instability disease caused by hypomorphic mutations in the *NBS1* gene encoding the Nbs1 (nibrin) protein. Nbs1 is a component of the Mre11/Rad50/Nbs1 (MRN) complex that acts as a sensor of double strand breaks (DSBs) in the DNA and is critical for proper activation of the broad cellular response to DSBs. Conditional disruption of the murine ortholog of *NBS1*, *Nbn*, in the CNS of mice was previously reported to cause microcephaly, severe cerebellar atrophy and ataxia. In this study we used MRI to study the brain morphology and organization of *Nbn* deleted mice. Using conventional T_2-weighted magnetic resonance, we found that the brains of the mutant mice (Nbs1-CNS-del) were significantly smaller than those of the wild-type animals, with marked mal-development of the cerebellum. Region of interest analysis of the T_2 maps revealed significant T_2 increase in the areas of white matter (corpus callosum, internal capsule and midbrain), with minor changes, if any, in gray matter. Diffusion tensor imaging (DTI) data confirmed that fractional anisotropy values were significantly reduced in these areas, mainly due to increased radial diffusivity (water diffusion perpendicular to neuronal fibers). Biochemical analysis showed low and dispersed staining for MBP and GalC in Nbs1-CNS-del brains, indicating defects in myelin formation and oligodendrocyte development. Myelin index and protein levels were significantly reduced in these brains. Our results point to a novel function of Nbs1 in the development and organization of the white matter.

Keywords: NBS; Nbs1 conditional knockout; MRI; White matter; Myelin; Oligodentrocytes

Introduction

Nijmegen breakage syndrome (NBS) is a rare autosomal recessive disorder characterized by microcephaly, mental deficiency, "bird-shaped" face, immunodeficiency, predisposition to lymphoreticular malignancies, chromosomal instability and radiation sensitivity (Chrzanowska et al., 1995; Digweed and Sperling, 2004; Seemanova et al., 1985; van der Burgt et al., 1996; Weemaes et al., 1981). NBS shares several features with another genomic instability syndrome, ataxia-telangiectasia (A-T) (Chun and Gatti, 2004; Crawford, 1998), but unlike A-T patients, NBS patients do not exhibit cerebellar ataxia and apraxic eye movements. NBS is caused by hypomorphic mutations in the *NBS1* gene, which encodes the Nbs1 (nibrin) protein (Carney et al., 1998; Varon et al., 1998). Nbs1, together with the Mre11 and Rad50 proteins, constitutes the NRM complex, a sensor of double strand breaks (DSBs) in the DNA (Petrini and Stracker, 2003; Stracker et al., 2004). The MRN

* Corresponding author. Department of Neurobiochemistry, Faculty of Life Sciences, Tel Aviv University, Tel Aviv, 69978, Israel. Fax: +972 3 6407168.
E-mail address: asafyan@zahav.net.il (Y. Assaf).

0014-4886/$ - see front matter © 2007 Elsevier Inc. All rights reserved.
doi:10.1016/j.expneurol.2007.09.021

complex is required for proper initiation of the DNA damage response by DSBs. Specifically, it is essential for the activation of the nuclear protein kinase ATM (Cerosaletti and Concannon, 2004; Horejsi et al., 2004; Paull and Lee, 2005; Uziel et al., 2003; Weitzman et al., 2003; You et al., 2005). ATM mobilizes the DSB response, an intricate signaling network that activates DNA repair, cell cycle checkpoints and numerous other signaling pathways by phosphorylating key players in this response (Bakkenist and Kastan, 2003; Elkon et al., 2004; Kurz and Lees-Miller, 2004; Shiloh, 2003, 2006).

NBS patients are highly sensitive to invasive radiation (Chrzanowska et al., 1995; Kruger et al., 2007; van der Burgt et al., 1996); thus, computed tomography, positron emission tomography and infra-red are extremely harmful for them. The few reports on invasive imaging of NBS subjects reported microcephaly, posterior cysts, hydrocephalus and other nonspecific observations (Der Kaloustian et al., 1996; Stoppa-Lyonnet et al., 1992; Taalman et al., 1989). Consequently, magnetic resonance imaging (MRI) and ultrasound (US), which are noninvasive imaging modalities, are the methods of choice for the diagnosis and follow-up of this disorder. Nevertheless, few studies have carried out MRI investigations of NBS patients (Bekiesinska-Figatowska et al., 2004, 2000); those that did reported abnormal development of frontal lobes, increased cerebro-spinal fluid volume, frequent cyst formation, microcephaly and malignant tumors. Aside from microcephaly and frontal lobe mal-development, MRI studies of NBS reported heterogeneous morphology of brain pathology.

Knocking out the murine homolog of *NBS* (*Nbn*) led to embryonic lethality (Dumon-Jones et al., 2003; Frappart et al., 2005; Zhu et al., 2001). Heterozygous animals ($Nbn^{+/-}$) developed malignant tumors and were sensitive to ionizing radiation (Dumon-Jones et al., 2003). Recently, conditional inactivation of *Nbn* in the central nervous system (CNS) was achieved using the nestin-Cre conditional gene targeting system (Frappart et al., 2005). These animals (Nbs1-CNS-del) presented with microcephaly, cerebellar mal-development and ataxia, reminiscent of the clinical presentation of NBS as well as advanced A-T. Thus, Nbs1-CNS-del mice represent a chromosomal instability disorder that resembles both diseases.

Here, we conducted an MRI study to characterize the appearance and integrity of various brain structures in Nbs1-CNS-del mice. Our study revealed that conditional *Nbn* inactivation led to impaired development of the white matter, pointing to novel pathophysiological roles of this gene and its protein product in neurodegenerative processes.

Methods

Animals

In vivo MRI and histology were performed on 9 Nbs1-CNS-del and 9 wild-type (Nbs1-CNS-ctrl) mice ~60 days old. The genetic background of these mice is a mix of 129/Sv and C57BL/6. At this age, Nbs1-CNS-del exhibited reduced body weight and severe cerebellar deficits. MRI scans were carried out under 1% isoflurane anesthesia and lasted 30 min, during which body temperature of the animals was kept at 37 °C using a warm water blanket, and respiration was monitored and kept around 30 breath cycles per min. Following MRI, the mice were euthanized and their brains prepared for histology. The experimental protocol was approved by the Tel Aviv University Committee for Experiments in Animals.

MRI

Mice of the two genotypes were scanned in a 7T/30 spectrometer (Bruker, Rheinstetten, Germany) using a 10 mm surface coil and 400 mT/m gradient system. The MRI protocol included multi-echo T_2-weighted images (TR = 3000, TE linearly incremented from 10 ms to 120 ms in 10 ms intervals) and diffusion-weighted echo planar images (DWI-EPI, TR/TE = 3000/25 ms, 4 EPI segments, $\Delta/\delta = 10/4.5$ ms, b value of 1000 s/mm^2 acquired at 16 noncollinear gradient directions). In all experiments the field of view (FOV) was 20×20 mm^2 with matrix dimensions of 192×160 (for the T_2 experiments) and 96×80 for the DWI-EPI. Eight slices of 1.2 mm thickness and no gap were acquired both in axial and sagittal orientations for the T_2 series, and in axial orientation only for the diffusion series.

Image analysis

The multi-echo T_2-weighted images were used to generate quantitative T_2 maps. The multi-echo signal was fitted to a mono-exponential decay function on a pixel-by-pixel basis to extract the T_2 value for each image pixel. The DWI-EPI data were analyzed using the DTI analysis framework (Basser and Pierpaoli, 1998; Pierpaoli and Basser, 1996; Pierpaoli et al., 1996) to produce the FA, ADC, $D_{//}$ and $D_{\perp}$. While ADC maps show an iso-intense signal in both gray matter and white matter, the FA maps are more specific to white matter and have a relatively high signal in white matter regions.

Region of interest analysis of the indexed maps (T_2, $D_{\perp}$, $D_{//}$, FA and ADC) was carried out by manual polygon segmentation on the following regions: olfactory bulb, V1/V2 cortical area, M1/S1 cortical area, hypothalamus, thalamus, hippocampus, the caudate-putamen complex, corpus callosum, midbrain, cotricospinal tract at the level of the interal capsule and cerebellar white matter. The two mouse genotypes were compared using Student's t-test.

Histology

After MRI, the animals were sacrificed and their brain was extracted and prepared for immunohistochemistry staining for myelin basic protein (MBP), cell nucleus (Sytox) and mature oligodendrocytes (GalC). At each of 4 time points – 1, 7, 15 and 60 days of age – two mice in this group were sacrificed and their cerebellar folia were stained for the aforementioned markers.

Tissue preparation

Mouse brains were dissected and fixed in 4% fixative (4% formaldehyde in PBS) for 24 h and placed in PBS. The brains

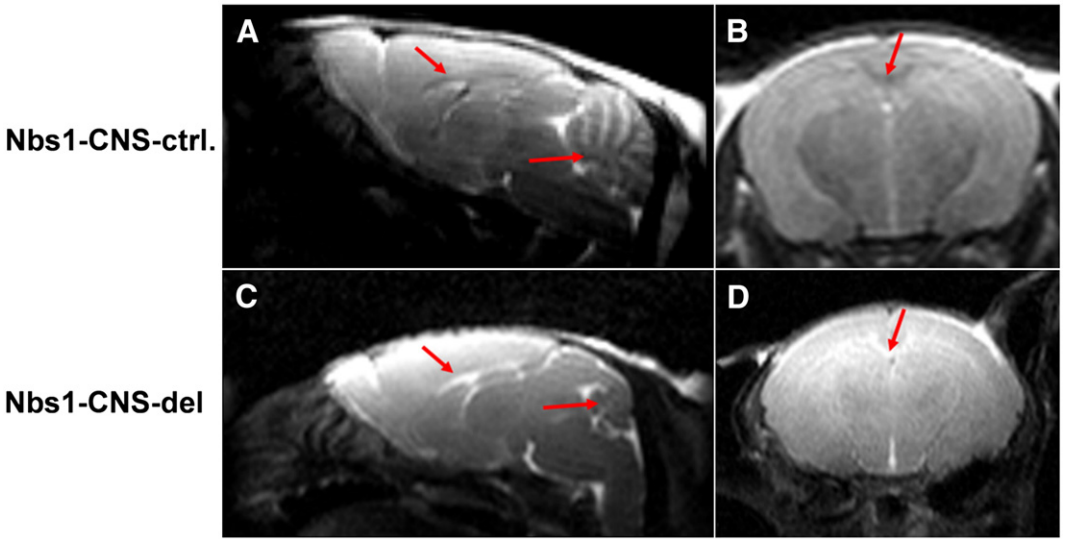

Fig. 1. T_2-weighted MRI in various *Nbn* genotypes. T_2-weighted MRI images (TE = 70 ms) are shown for Nbs1-CNS-ctrl (A in axial orientation and B in saggital orientation) and Nbs1-CNS-del (C in axial orientation and D in saggital orientation). Arrows point to the corpus callosum in the coronal sections and the corpus callosum and cerebellar white matter in the saggital sections. The typical hypointensity of the corpus callosum in wild-type mice is not observed in the Nbs1-CNS-del animals where it is replaced by hyperintense signal.

were then infiltrated for cryo-protection with 4% sucrose (Merck, city, country) for 2 h at 4 °C, followed by 20% sucrose plus 5% glycerol (Merck) in PBS overnight at the same temperature. Fixed brains were embedded in Tissue Freezing Medium (Leica Instruments GmbH, Nussloch, Germany) and quickly frozen in liquid nitrogen. Cross-sections (10 μm) were placed on subbed slides (0.5% gelatin, containing 0.05% chromium potassium sulfate) and stored at 20 °C.

Immunohistochemical analysis

Sections were washed in PBS for 30 min and blocked with 1% bovine serum albumin (BSA) (Sigma, St. Louis, MO) and 10% normal donkey serum (NDS) (Jackson ImmunoResearch, Baltimore, MD) in PBS for 1 h at room temperature. The sections were incubated overnight with the primary antibody, as specified, in 0.25% Triton X100 (Sigma, St. Louis, MO) at 4 °C. The slides were washed three times with PBS and incubated with the secondary antibody for 1 h at room temperature. After being washed once with PBS and twice in a buffer containing Tris (10 mM; Sigma) EDTA (1 mM; Merck), the sections were incubated with the nucleic acid dye Sytox blue (Molecular Probes, Invitrogen, Carlsbad, Germany) for 30 min. Slides were then washed three times with the same buffer and mounted with aqueous mounting medium containing anti-fading agents (Biomeda, Burlingame, CA). Observations and photography were carried out with a Zeiss (Oberkochen, Germany) LSM 510 confocal microscope.

Western blot analysis

Western blot analysis was performed as described by Harlow and Lane using 10% polyacrylamide gels. Each lane was loaded with an equal amount of protein extracts, which, following electrophoresis, were transferred to an immobilon polyvinylidene disulfide (PVDF) membrane (Millipore, Billerica, MA) for 1.5 h. Blots were stained with Ponceau to verify equal loading and transfer of proteins, and incubated with 5% low-fat milk in buffer TBST (Tris 20 mM, NaCl 150 mM, 1% Tween 20, Sigma) for 1 h. Membranes were then probed with polyclonal anti-myelin basic protein (MBP) antibody (1:1000, washed three times with 5% low-fat milk in TBST, and incubated with anti-rabbit IRDye 800CW secondary antibody (1:10,000; LI-COR, Lincoln, NE). The intensity of the signal was determined using the Odyssey infrared imaging system (LI-COR, Lincoln, NE).

Electron microscopy

Mice were perfused with 4% gluteraldehyde in 0.1 M cacodilate buffer (pH 7.4). 100 μm blocks were cut from the corpus callosum and from the white matter of the cerebellum, rinsed in cacodilate buffer, post-fixed in 1% OsO4 in PBS and washed again. After dehydratation in graded ethanol solution, the tissues were embedded in glycid ether 100 (Serva, Heidelberg, Germany). Ultra-thin sections (~0.1 μm) were stained with uranyl acetate and lead citrate and examined in Jeol 1200 EX TEM (Tokyo, Japan).

We chose the cerebellar white matter for this analysis because the cerebellum is believed to be the primary CNS structure affected in this model, and is the most studied CNS organ in chromosomal instability disorders.

Results

MRI

T_2-weighted MRI revealed significant differences in morphology and image contrast changes between the Nbs1-CNS-

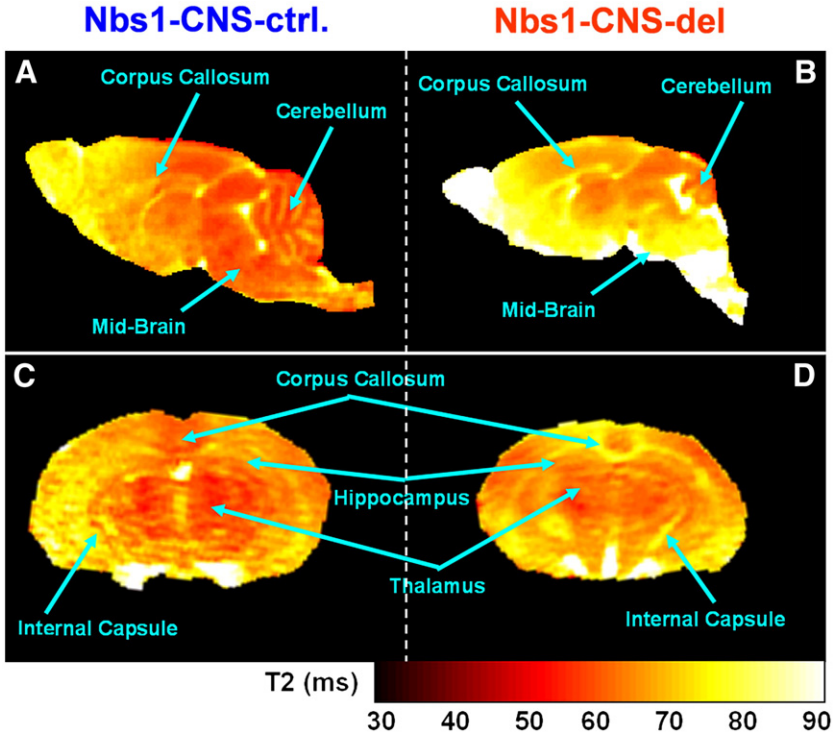

Fig. 2. Quantitative T_2 analysis. T_2 maps in saggital (A and B) and axial (C and D) orientations of Nbs1-CNS-ctrl (left, A and C) and Nbs1-CNS-del mice (right, B and D). The color-scale represents the T_2 values in milliseconds (ms) as indicated in the color bar below the image. Arrows point to regions where significant differences are observed between the two groups, such as the corpus callosum, midbrain and internal capsule, and regions where the differences are more subtle—thalamus and hippocampus. (For interpretation of the references to colour in this figure legend, the reader is referred to the web version of this article.)

del and Nbs1-CNS-ctrl genotypes. First, the brains of the former were significantly smaller (microcephalic) than those of the latter, with prominent mal-development of the cerebellum (Fig. 1). Interestingly, the width of the cerebral cortex was significantly smaller in Nbs1-CNS-del (1.26±0.15 mm) compared to wild-type animals (1.84±0.17 mm) ($p<0.001$). In addition, the typical hypointense white matter signal (as observed in Nbs1-CNS-ctrl brains) in the corpus callous, internal-capsule and cerebellar folia almost disappeared in Nbs1-CNS-del animals (red arrows in Fig. 1) and was replaced by abnormal hyperintense signal in those regions. These qualitative observations were further characterized by calculating the T_2 values in each image voxel, followed by ROI analysis. T_2 maps (Fig. 2) show diffuse changes across the brain, with most significant changes in the corpus callousm, internal capsule and cerebellum. Typical T_2 values in regions of white matter in Nbs1-CNS-ctrl mice were about 60 ms, whereas values in similar regions in Nbs1-CNS-del mice reached 80 ms. ROI analysis of the T_2 maps supported this observation: T_2 was significantly increased in areas of white matter (corpus callosum, internal capsule and mid brain) and changes, if any, were minor in gray matter regions (Table 1). The most significant change in white matter regions was in the corpus callosum where there was a 14% increase. A slight increase in T_2 was also found in the hippocampus (~6%), which was the only gray matter region to show a significant trend of T_2 changes.

White matter changes observed in the T_2 analysis were also studied by DTI, an advanced MRI application that provides unique and more specific information on white matter (Basser and Pierpaoli, 1998, 1996; Pierpaoli et al., 1996). Four indices are extracted from DTI: fractional anisotropy (FA), parallel diffusivities ($D_{//}$) and radial diffusivities ($D_{\perp}$) (in relation to white matter fiber axis, i.e., parallel and perpendicular to the neuronal fibers), and apparent diffusion coefficient (ADC). Neurodegenerative processes are usually accompanied by increased ADC, increased radial diffusivity and reduced FA.

DTI analysis revealed widespread white matter damage in Nbs1-CNS-del mice (Fig. 3). FA was significantly reduced in all measured regions (Fig. 3 and Table 2). The FA reduction was mainly due to increased radial diffusivity (Fig. 3 and Table 2).

Table 1
ROI analysis of T_2 maps in Nbs1-CNS-ctrl and Nbs1-CNS-del mice

Area	Nbs1-CNS-ctrl	Nbn-CNS-del	*p*-value (Student's *t*-test)
Olfactory bulb	72.1±3.5 ms	75.5±3.9 ms	n.s.
V1/V2 cortical area	64.6±3.5 ms	66.1±2.5 ms	n.s.
M1/S1 cortical area	64.5±2.4 ms	65.9±1.6 ms	n.s.
Hypothalamus	67.0±3.1 ms	67.8±4.1 ms	n.s.
Thalamus	63.2±2.1 ms	62.1±2.8 ms	n.s.
Caudate-putamen	67.4±2.6 ms	69.4±3.8 ms	n.s.
Hippocampus	64.9±2.6 ms	68.5±3.7 ms	<0.05
Corpus callosum	62.1±2.0 ms	70.8±2.5 ms	<0.0001
Midbrain	60.7±2.2 ms	65.1±3.3 ms	<0.0005
Cotrico-spinal tract	72.1±3.5 ms	75.5±3.9 ms	<0.0005
Cerebellar white matter	60.4±1.8 ms	65.1±3.3 ms	<0.01

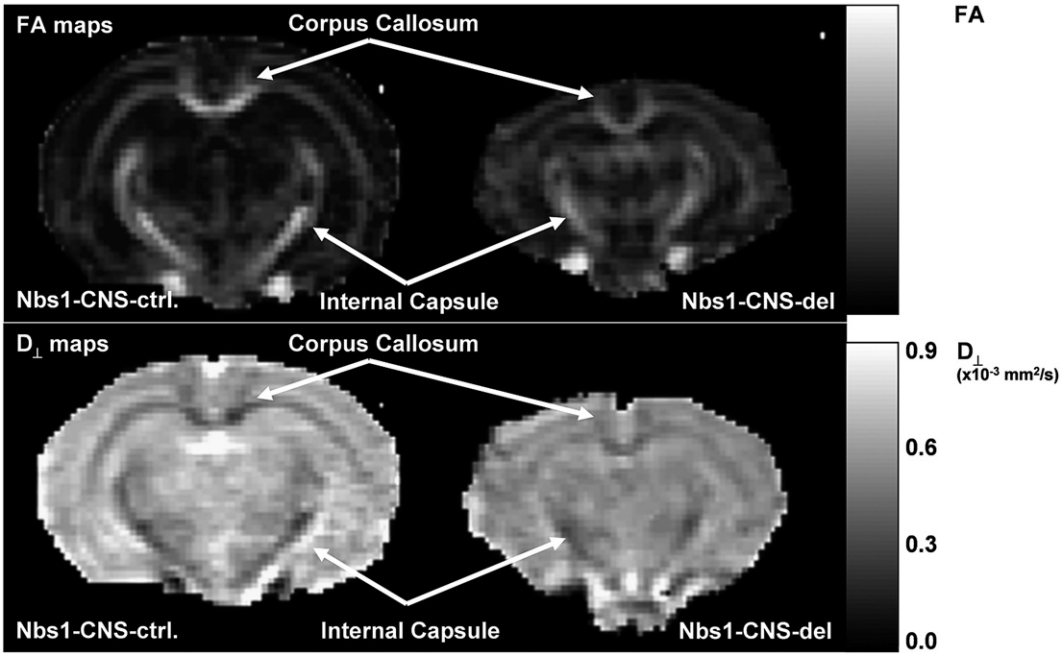

Fig. 3. White matter analysis from diffusion MRI. Diffusion tensor imaging (DTI) analysis of Nbs1-CNS-ctrl (left) and Nbs1-CNS-del (right) animals. FA maps (A and B) show high signal in areas of white matter (corpus callosum and internal capsule), depicting loss of intensity in these regions in Nbs1-CNS-del mice (B). Perpendicular diffusivity ($D_\perp$) shows hypointense signal in areas of white matter in the Nbs1-CNS-ctrl mice (C), which is less evident in the Nbs1-CNS-del mice (D), indicating an elevation of this index in the mutant animals.

FA was the most sensitive parameter, showing more than a 20% reduction in the mutant animals, and all regions with cerebellar white matter were most affected, with a 33% reduction in FA. Changes in FA are a consequence of changes in the radial and parallel diffusivities, from which it is calculated. The parallel diffusivity showed a decrease trend that was significant only in the corpus callosum and the midbrain, while the radial diffusivity was significantly increased in all regions of mutant brains, with the internal capsule showing the most striking change of over 60%. As a result, the ADC, which is a weighted average of the radial and parallel diffusivities, showed nonsignificant changes in all regions. Numerical data are summarized in Table 2.

Table 2
ROI analysis of diffusion indices in Nbs1-CNS-ctrl and Nbs1-CNS-del mice

Area		Nbs1-CNS-ctrl	Nbs1-CNS-del	*p*-value (Student's *t*-test)
Corpus callosum	FA	0.52±0.05	0.40±0.04	<0.005
	ADC*	0.74±0.03	0.70±0.04	n.s.
	$D_{/\!/}$*	1.21±0.13	1.01±0.09	<0.05
	$D_\perp$*	0.39±0.01	0.43±0.02	<0.001
Midbrain	FA	0.63±0.05	0.43±0.04	<0.0005
	ADC*	0.74±0.08	0.72±0.07	n.s.
	$D_{/\!/}$*	1.36±0.12	1.08±0.18	<0.05
	$D_\perp$*	0.31±0.06	0.44±0.05	<0.05
Cotrico-spinal tract	FA	0.66±0.05	0.50±0.04	<0.005
	ADC*	0.67±0.07	0.69±0.03	n.s.
	$D_{/\!/}$*	1.26±0.13	1.11±0.08	n.s.
	$D_\perp$*	0.26±0.06	0.40±0.04	<0.005
Cerebellar white matter	FA	0.36±0.04	0.24±0.03	<0.005
	ADC*	0.67±0.04	0.69±0.07	n.s.
	$D_{/\!/}$*	0.95±0.05	0.85±0.09	n.s.
	$D_\perp$*	0.45±0.04	0.53±0.05	<0.05

*ADC, $D_{/\!/}$ and $D_\perp$ are indicated with the units of $\times 10^{-3}$ mm^2/s.

Histology

One of the major neurological signs of Nbs1-CNS-del mice is ataxia, which is often associated with cerebellar pathology. Thus, histological analysis focused on the cerebellar white matter regions. At the age of 2 months, Nbs1-CNS-del mice showed low and dispersed staining for myelin basic protein (MBP), an important component of the myelin sheath. In contrast, the Nbs1-CNS-ctrl cerebella showed positive staining for MBP, with ordered fiber-like arrangement along the folia spreading into the zone of the cell bodies (evidenced by Sytox staining). Nbs1-CNS-del mice displayed mainly cell body staining and only small traces of the arranged fibers (Fig. 4).

Staining with MBP was done at different developmental stages to trace the origin of the white matter changes. On postnatal day 1, the myelin could be observed in Nbs1-CNS-del mice in the vicinity of the Purkinje cells. While in wild-type cerebella the myelin was gradually formed during development around the area of the white matter, no such developmental pattern was observed in Nbs1-CNS-del cerebella: the myelin was disorganized and the characteristic structures of the cerebellar white matter were not observed, even on day 15 when the cerebellum is at an advanced developmental stage (Fig. 4). Western blotting analysis of cerebellar and cerebral protein extracts for MBP levels was performed to confirm the

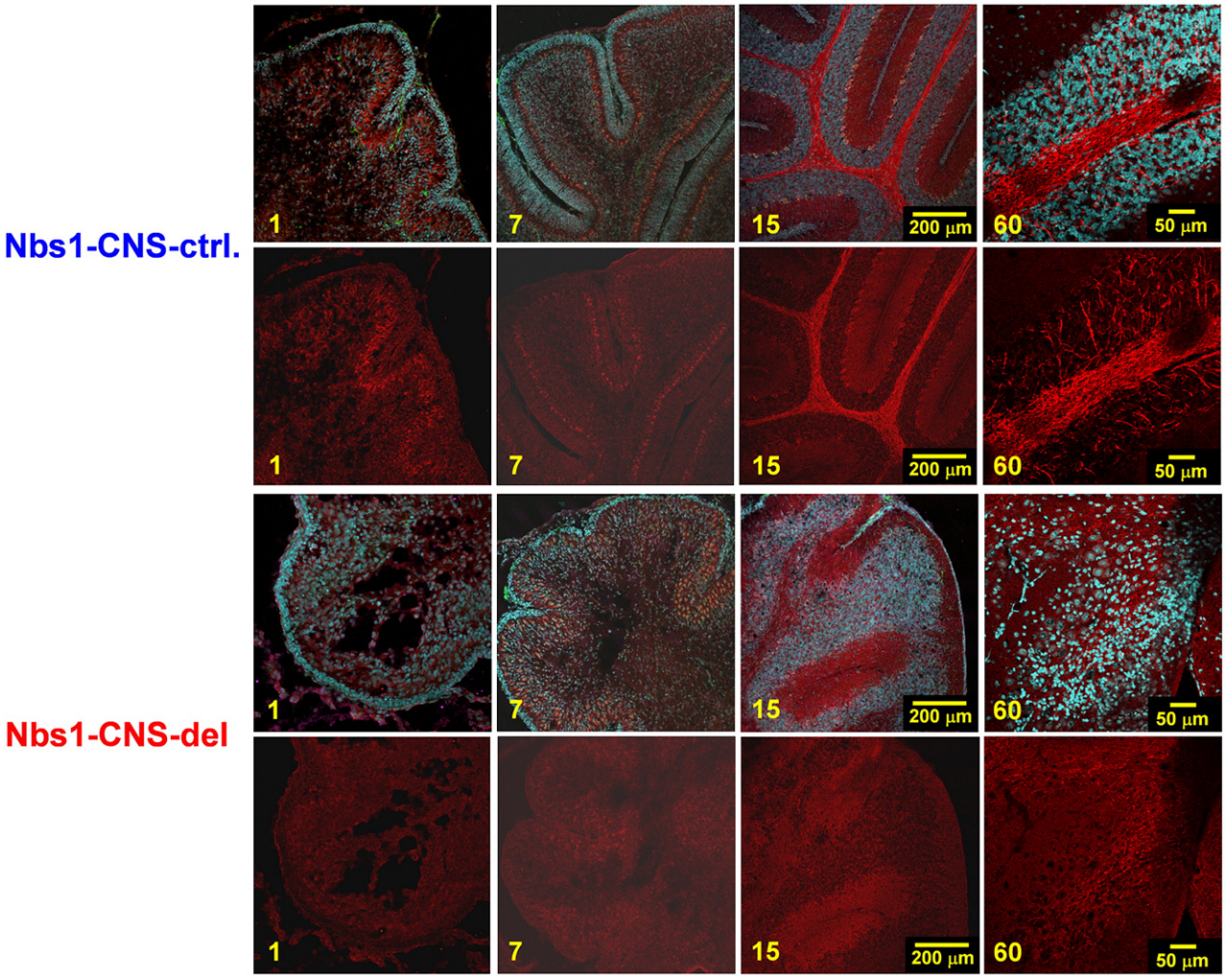

Fig. 4. Development of the cerebellar white matter. Cerebellar sections were prepared from the two genotypes on postnatal days 1, 7, 15 and 60, stained with the anti-MBP antibody that labels the myelin, and co-stained with Sytox blue that labels cell nuclei. (For interpretation of the references to colour in this figure legend, the reader is referred to the web version of this article.)

MRI and immunohistochemical analyses of the white matter integrity. Fig. 5 shows a marked reduction in cerebellar MBP levels in the mutant mice.

Since myelin sheaths are formed by oligodendrocytes, we studied the morphology and organization of oligodendrocytes in the cerebella of the two genotypes at 1, 7, 15 and 60 days of age. Marginal oligodendrocyte staining with the marker GalC was seen in Nbs1-CNS-ctrl brains on days 1 and 7, became significant at 15 days and much stronger at 60 days (Fig. 6). By contrast, *Nbn* inactivation severely impaired the migration and organization of these cells, and the brains of the mutant mice showed no positive staining with GalC between 1 and 60 days after birth (Fig. 6), indicating abnormal development of oligodendrocytes.

Electron microscopy analysis of corpus callosum and cerebellar samples from the two animal genotypes were carried out to visualize the change at subcellular levels. Wild-type mice showed the typical ordered arrangement of packed axons thickly wrapped by myelin (Fig. 7A), while the axons in Nbs1-CNS-del mice were significantly enlarged, loosely packed and wrapped by thin layers of myelin (Fig. 7B). The myelin index (the thickness of the axon's outer diameter divided by its inner diameter) showed a significant reduction in Nbs1-CNS-del cerebellum (60%) and corpus callosum (55%) compared to wild-type tissues (Fig. 7C).

Discussion

This study has demonstrated that CNS conditional knock-out of the *Nbn* gene causes major mal-development of the white matter in mice. Since the Nbs1 protein is involved in the cellular response to DSBs, our results suggest that oligodendrocytes might be particularly vulnerable to abrogation of the DSB response. Importantly, conventional MRI markers (T_2, ADC) and white matter markers (FA, $D_\perp$) did not detect gray matter damage in Nbs1-deficient brains although significant microcephaly was observed. On the other hand, white matter damage was consistently observed, evidenced by elevated T_2, decreased FA and increased $D_\perp$, which are typical of white matter neurodegenerative diseases (Stark and Bradley, 1992; Tofts,

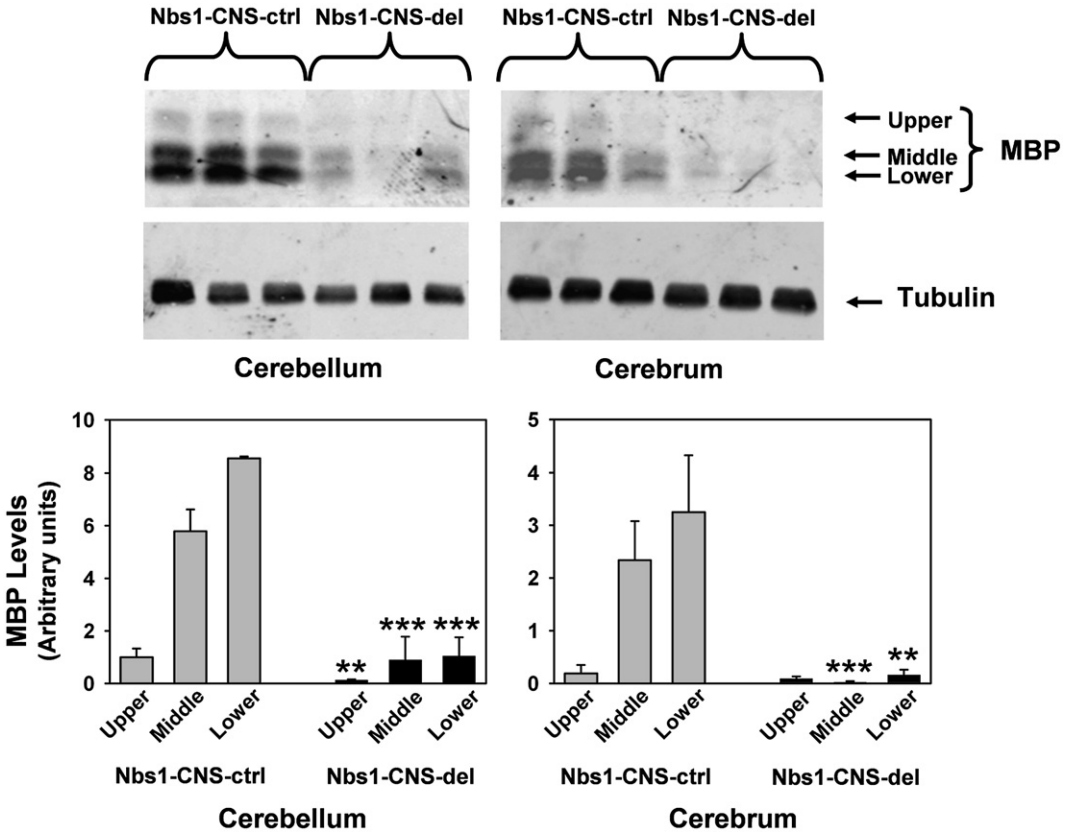

Fig. 5. Reduced levels of MBP in Nbs1-CNS-del brains. (A) Western blotting analysis of total protein extracts from cerebrum and cerebellum of the indicated genotypes after immunoreaction with the anti-MBP antibody. The antibody recognizes 3 different proteins with molecular weights ranging from 14 to 21 kDa. In order to compare protein amounts in the different lanes, the blots were stripped and reacted with an anti-tubulin antibody. (B) Quantitative analysis of bands using the Odyssey software and normalized against the corresponding tubulin readings. MBP levels were quantified by analysis of all three bands. Data are from four animals were averaged for each genotype.

2002). Our study thus provides the first evidence that Nbs1 is important for the development of the white matter.

Oligodendrocyte vulnerability and DNA damage response

We show here that defective DSB response caused by knock-out of *Nbn* in the CNS causes, *inter alia*, significant damage to the white matter and abrogates oligodendrocyte development. Oligodendrocytes are extremely vulnerable cells (McQuillen et al., 2003; Merrill and Scolding, 1999). During development they are the last to develop and during aging they are the first to degenerate (Peters, 2002). Being responsible for the formation of myelin that wraps the axons and ensures fast and efficient electrical transmission, oligodendrocytes are crucial for normal CNS development. Several inherited developmental disorders originate from abnormal white matter development, including Pelizaeus-Merzbacher disease, X-linked adrenoleukodystrophy, Canavan disease and vanishing white matter diseases (Di Rocco et al., 2004; Kaye, 2001; Merrill and Scolding, 1999; Noetzel, 2004). Each of these disorders is characterized by abnormal oligodendrocyte and myelin metabolism, which usually leads to demyelination, hypomyelination or dismyelination. Generic disorders affecting myelin directly are induced by mutations in genes encoding structural myelin proteins (e.g., PLP and MBP), myelin-related regulatory proteins or proteins involving lipid metabolism (Di Rocco et al., 2004; Kaye, 2001; Merrill and Scolding, 1999). The common phenotype in all these conditions is neurological deficit, especially of the motor system (ataxia, trembling, paralysis, etc.) as seen in the Nbs1-CNS-del model (Frappart et al., 2005).

MRI appearance of white matter damage in Nbs1-CNS-del mice brains

MRI measures the physical behavior of water molecules. T_2, the most basic contrast mechanism in MRI, measures the transverse relaxation time of water molecules in tissue (Stark and Bradley, 1992; Tofts, 2002); it is long in fluids and short in dense tissue. The assumption is that T_2 is correlated with water content (Stark and Bradley, 1992; Tofts, 2002), making an increase in T_2 the expression of a degenerative process. We found increased T_2 in white matter but not gray matter in Nbs1-CNS-del mice. The increased T_2 relaxation time together with hyperintense signals strongly suggests that the myelin in Nbs-CNS-del animals is impaired, but it tells nothing about the nature of the impairment. DTI and its indices (FA, ADC and $D_\perp$), on the other hand, are more specific as they measure the translational motion of water molecules (Basser and Pierpaoli, 1998; Pierpaoli and Basser, 1996; Pierpaoli et al., 1996), making them more informative about white matter pathology. While ADC provides the averaged

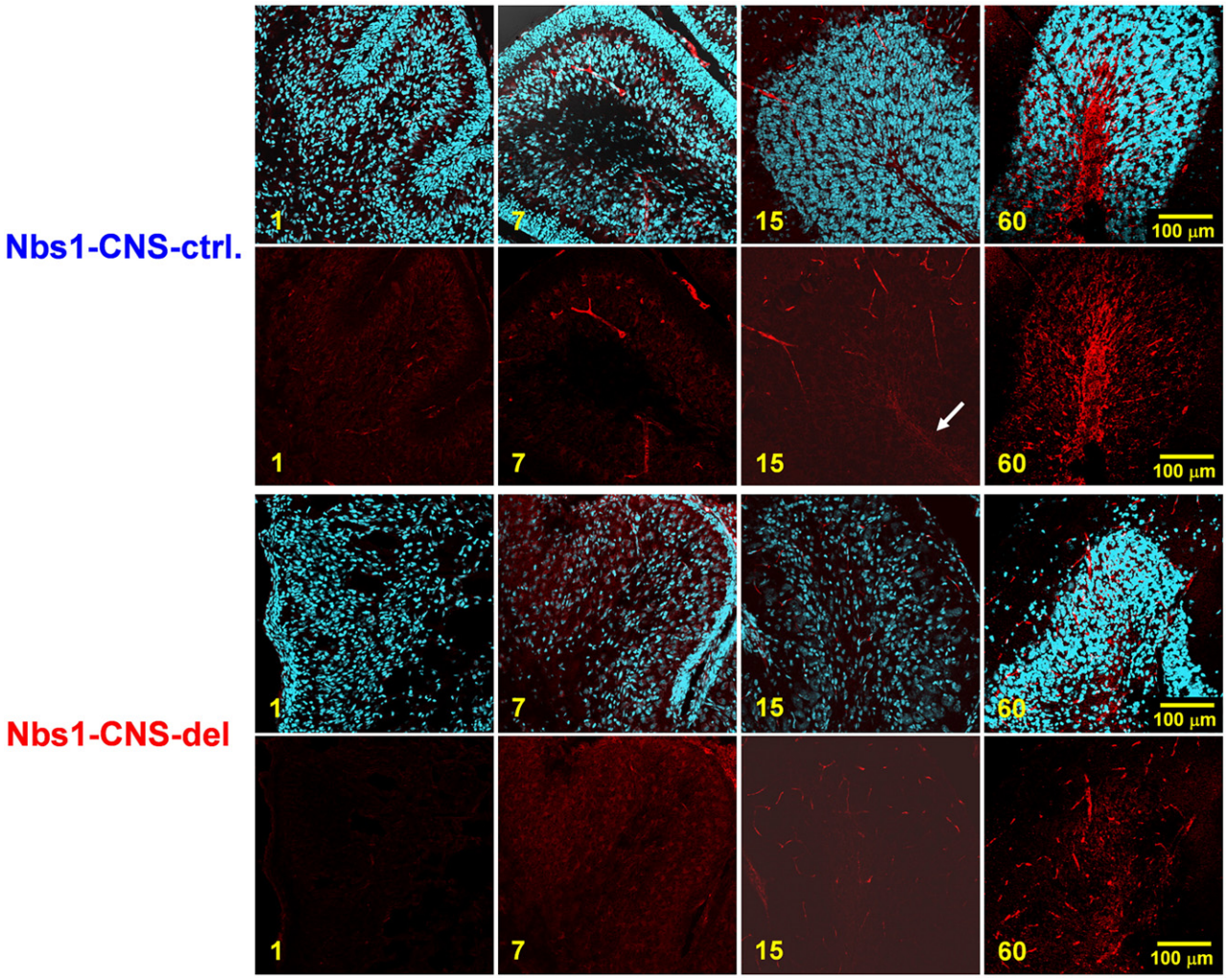

Fig. 6. Late stages of oligodentrocyte development in Nbs1-CNS-ctrl and Nbs1-CNS-del cerebella. Cerebellar sections of the indicated genotypes made on postnatal days 1, 7, 15 and 60 days were reacted with an anti-GalC antibody that labels mature oligodentrocytes, and co-stained with Sytox blue that labels cell nuclei. At day 15 the white matter contains mossy fibers, climbing fibers and Purkinje cell axons that reach the deep nuclei (white arrow). Fully mature, well-organized white matter can be observed in 60-day-old Nbs1-CNS-ctrl mice, while Nbs1-CNS-del mice exhibit only sparse staining in the cerebellum at all time points. (For interpretation of the references to colour in this figure legend, the reader is referred to the web version of this article.)

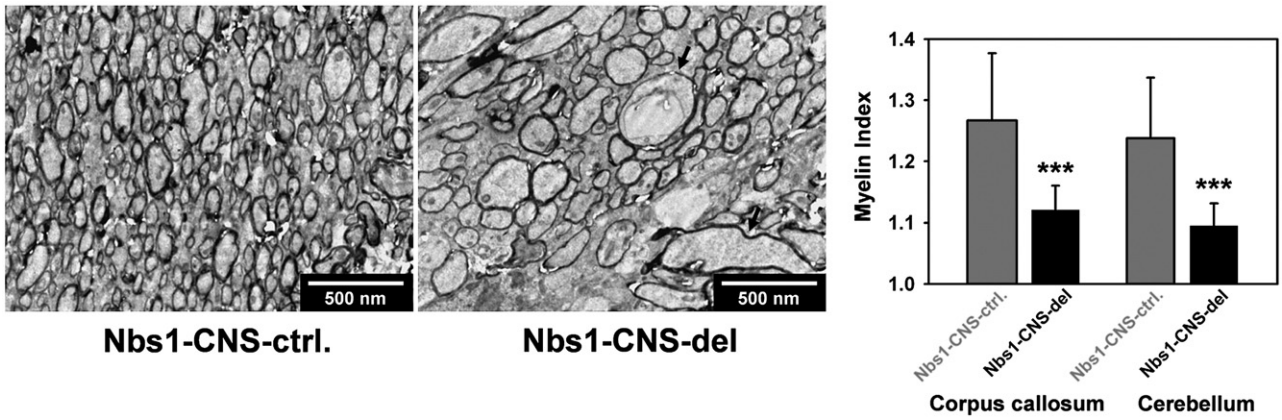

Fig. 7. Morphological appearance of axons. Electron microscopy sections through the corpus callosum of Nbs1-CNS-ctrl (A) and Nbs1-CNS-del (B) mice showing differences between them in axonal density, myelin thickness, and axonal diameter. (C) According to the myelin index analysis, calculated as the outer diameter including the myelin sheath divided by the inner diameter of the axons without the myelin, Nbs1-(CNS)-del mice show values closer to 1, indicating pathological hypomyelination.

3-dimensional diffusion coefficient and does not show specific contrast to gray or white matters, FA and $D_{\perp}$ provide more specific information on white matter and enhance the MRI sensitivity in this tissue. FA measures the motional anisotropy of water molecules in the tissue: this anisotropy is high in white matter because the motion of water molecules is fast along the fibers and perturbed perpendicular to them (Basser and Pierpaoli, 1998; Pierpaoli and Basser, 1996; Pierpaoli et al., 1996). Using DTI, it is possible to estimate the diffusion parallel and perpendicular to the fibers ($D_{//}$ and $D_{\perp}$) and the normalized differences between them (FA). In most neurological disorders affecting the white matter, $D_{\perp}$ increase is accompanied by FA decrease (Mori and Zhang, 2006; Neil et al., 2002; Sundgren et al., 2004), indicating either loss of fibers or demyelination but without being able to differentiate between the two processes. We observed significant changes of the FA and $D_{\perp}$ values in the Nbs1-CNS-del mouse brain that were widespread in all white matter regions, indicative of white matter pathology.

The magnitude of FA reduction should be correlated with loss of the white matter's micro-structure. In contrast to some white matter disorders (such as ALD) where myelin breakdown causes FA reduction by ~80% (Ito et al., 2001), our mouse model shows lower but still highly significant reduction, ~30%. This indicates that there is still some ordered structure of neuronal fibers in the white matter of Nbs1-CNS-del mice. Electron microscopy examination supported this MRI result, demonstrating large axons with low numbers of myelin wraps around them (see Fig. 7).

Implications for chromosomal instability disorders

Nbs1-CNS-del does not completely mimic the phenotypic pathology of NBS (Frappart et al., 2005), since NBS in humans is caused by hypomorphic mutations while the Nbs1-CNS-del mice completely lack the Nbs1 protein in their CNS. Indeed, in the few studies on MRI patterns in NBS patients, no specific damage to the white matter was reported (Bekiesinska-Figatowska et al., 2004, 2000). It is possible that the hypomorphic nature of the human *NBS1* mutations does not lead to the full-blown tissue damage that might have been caused by null *NBS1* alleles in humans. Interestingly, in certain respects the mouse phenotype is closer to that of human A-T patients as it includes marked cerebellar pathology and ataxia, making it a better animal model for cerebellar pathology caused by defective DSB response than *Atm*-knockout mice, which do not mimic the cerebellar pathology typical of A-T (Barlow et al., 1996). Because the cerebellum is often affected in the human forms of genomic instability disorders, most of the previous work on the Nbs1-CNS-del mice and on other mouse models of these disorders focused on the cerebellar pathologies associated with these disorders (Oka and Takashima, 1998; Taylor and Byrd, 2005; Watters, 2003); the pathophysiology of the white matter and axonal trajectories was often disregarded. The present study points to the importance of white matter and axonal trajectories as a possible focus of pathology in chromosomal instability syndromes; and the capability of MRI to identify and quantify damage to these tissues. Indeed, there is evidence in the literature of white matter damage in the MRI scans of A-T patients (Chung et al., 1994; Ciemins and Horowitz, 2000; Demaerel et al., 1992; Firat et al., 2005), although it did not appear in all subjects and can not be considered a specific phenotype of A-T.

Although MRI detected white matter damage in the Nbs1-CNS-del mice, it is unclear whether the white matter defects are directly involved in the microcephaly and neurological deficits in these animals, or are secondary to more global tissue pathology. Notably, however, the neurological deficits seen in Nbs1-CNS-del mice and in human genomic instability disorders are observed in other myelin-related disorders, suggesting that white matter damage may play a significant role in the neurological symptoms of chromosomal instability disorders. Immunohistological analyses of MBP and GalC in our study revealed abnormal development of the myelin and oligodendrocytes, suggesting that the abnormal myelin might be due to maldevelopment of oligodendrocytes (Figs. 4–7). Electron microscopy supported these observations.

Nbs1-CNS-del mice as a model of neurodegenerative diseases

Neurodegenerative diseases are generally characterized by impaired functionality of the brain, which can be assessed by the total inputs and outputs of neuronal circuits. Specific disorders involve deregulation of specific neuronal circuits and populations. Brain functionality is influenced by parameters such as the number of cells in specific neuronal circuits, interactions among neuronal cells, interactions among different neuronal circuits, level of organization of each circuit and functionality of the cells and their environmental in each circuit. Reduction in the myelin index such as that observed in our nbs1-CNS-del mice implies a marked reduction in electrical activity of various neuronal circuits—an important determinant of brain functionality. Our and previous findings collectively suggest that inactivation of the *Nbn* gene in the CNS leads to marked reduction in the amount of cerebellar granule neurons, disruption of neuronal cell organization, especially cerebellar Purkinje cells and severe impairment of the white matter. Thus, elimination of a DNA damage response protein has a profound effect on brain structure and functionality, further underscoring the critical role of this response in CNS development.

Acknowledgments

The MRI scanner used in this study was purchased with a grant from The Israel Science Foundation and operated under the Raymond and Beverly Sackler Center for Biophysics, Tel Aviv University and The Alfredo Federico Strauss Center for Computational Neuro-Imaging, Tel Aviv University. This work was supported by research grants from the A-T Children's Project, the Israel Science Foundation and the US-Israel Binational Science Foundation (to A.B.), and The A-T Medical Research Foundation, The A-T Children's Project, the A-T Medical Research Trust and the A-T Ease Foundation (to Y.S.). ZQW is supported by the Association for International Cancer Research (AICR) UK.

References

Bakkenist, C.J., Kastan, M.B., 2003. DNA damage activates ATM through intermolecular autophosphorylation and dimer dissociation. Nature 421, 499–506.

Barlow, C., Hirotsune, S., Paylor, R., Liyanage, M., Eckhaus, M., Collins, F., Shiloh, Y., Crawley, J.N., Ried, T., Tagle, D., Wynshaw-Boris, A., 1996. Atm-deficient mice: a paradigm of ataxia telangiectasia. Cell 86, 159–171.

Basser, P.J., Pierpaoli, C., 1998. A simplified method to measure the diffusion tensor from seven MR images. Magn. Reson. Med. 39, 928–934.

Bekiesinska-Figatowska, M., Chrzanowska, K.H., Sikorska, J., Walecki, J., Krajewska-Walasek, M., Jozwiak, S., Kleijer, W.J., 2000. Cranial MRI in the Nijmegen breakage syndrome. Neuroradiology 42, 43–47.

Bekiesinska-Figatowska, M., Chrzanowska, K.H., Jurkiewicz, E., Wakulinska, A., Rysiewskis, H., Gladkowska-Dura, M., Walecki, J., 2004. Magnetic resonance imaging of brain abnormalities in patients with the Nijmegen breakage syndrome. Acta Neurobiol. Exp. (Wars.) 64, 503–509.

Carney, J.P., Maser, R.S., Olivares, H., Davis, E.M., Le Beau, M., Yates III, J.R., Hays, L., Morgan, W.F., Petrini, J.H., 1998. The hMre11/hRad50 protein complex and Nijmegen breakage syndrome: linkage of double-strand break repair to the cellular DNA damage response. Cell 93, 477–486.

Cerosaletti, K., Concannon, P., 2004. Independent roles for nibrin and Mre11-Rad50 in the activation and function of Atm. J. Biol. Chem. 279, 38813–38819.

Chrzanowska, K.H., Kleijer, W.J., Krajewska-Walasek, M., Bialecka, M., Gutkowska, A., Goryluk-Kozakiewicz, B., Michalkiewicz, J., Stachowski, J., Gregorek, H., Lyson-Wojciechowska, G., et al., 1995. Eleven Polish patients with microcephaly, immunodeficiency, and chromosomal instability: the Nijmegen breakage syndrome. Am. J. Med. Genet. 57, 462–471.

Chun, H.H., Gatti, R.A., 2004. Ataxia-telangiectasia, an evolving phenotype. DNA Repair (Amst) 3, 1187–1196.

Chung, E.O., Bodensteiner, J.B., Noorani, P.A., Schochet Jr., S.S., 1994. Cerebral white-matter changes suggesting leukodystrophy in ataxia telangiectasia. J. Child Neurol. 9, 31–35.

Ciemins, J.J., Horowitz, A.L., 2000. Abnormal white matter signal in ataxia telangiectasia. AJNR Am. J. Neuroradiol. 21, 1483–1485.

Crawford, T.O., 1998. Ataxia telangiectasia. Semin. Pediatr. Neurol. 5, 287–294.

Demaerel, P., Kendall, B.E., Kingsley, D., 1992. Cranial CT and MRI in diseases with DNA repair defects. Neuroradiology 34, 117–121.

Der Kaloustian, V.M., Kleijer, W., Booth, A., Auerbach, A.D., Mazer, B., Elliott, A.M., Abish, S., Usher, R., Watters, G., Vekemans, M., Eydoux, P., 1996. Possible new variant of Nijmegen breakage syndrome. Am. J. Med. Genet. 65, 21–26.

Di Rocco, M., Biancheri, R., Rossi, A., Filocamo, M., Tortori-Donati, P., 2004. Genetic disorders affecting white matter in the pediatric age. Am. J. Med. Genet. B. Neuropsychiatr. Genet. 129, 85–93.

Digweed, M., Sperling, K., 2004. Nijmegen breakage syndrome: clinical manifestation of defective response to DNA double-strand breaks. DNA Repair (Amst.) 3, 1207–1217.

Dumon-Jones, V., Frappart, P.O., Tong, W.M., Sajithlal, G., Hulla, W., Schmid, G., Herceg, Z., Digweed, M., Wang, Z.Q., 2003. Nbn heterozygosity renders mice susceptible to tumor formation and ionizing radiation-induced tumorigenesis. Cancer Res. 63, 7263–7269.

Elkon, R., Zeller, K.I., Linhart, C., Dang, C.V., Shamir, R., Shiloh, Y., 2004. In silico identification of transcriptional regulators associated with c-Myc. Nucleic Acids Res. 32, 4955–4961.

Firat, A.K., Karakas, H.M., Firat, Y., Yakinci, C., 2005. Quantitative evaluation of brain involvement in ataxia telangiectasia by diffusion weighted MR imaging. Eur. J. Radiol. 56, 192–196.

Frappart, P.O., Tong, W.M., Demuth, I., Radovanovic, I., Herceg, Z., Aguzzi, A., Digweed, M., Wang, Z.Q., 2005. An essential function for NBS1 in the prevention of ataxia and cerebellar defects. Nat. Med. 11, 538–544.

Horejsi, Z., Falck, J., Bakkenist, C.J., Kastan, M.B., Lukas, J., Bartek, J., 2004. Distinct functional domains of Nbs1 modulate the timing and magnitude of ATM activation after low doses of ionizing radiation. Oncogene 23, 3122–3127.

Ito, R., Melhem, E.R., Mori, S., Eichler, F.S., Raymond, G.V., Moser, H.W., 2001. Diffusion tensor brain MR imaging in X-linked cerebral adrenoleukodystrophy. Neurology 56, 544–547.

Kaye, E.M., 2001. Update on genetic disorders affecting white matter. Pediatr. Neurol. 24, 11–24.

Kruger, L., Demuth, I., Neitzel, H., Varon, R., Sperling, K., Chrzanowska, K.H., Seemanova, E., Digweed, M., 2007. Cancer incidence in Nijmegen breakage syndrome is modulated by the amount of a variant NBS protein. Carcinogenesis 28, 107–111.

Kurz, E.U., Lees-Miller, S.P., 2004. DNA damage-induced activation of ATM and ATM-dependent signaling pathways. DNA Repair (Amst.) 3, 889–900.

McQuillen, P.S., Sheldon, R.A., Shatz, C.J., Ferriero, D.M., 2003. Selective vulnerability of subplate neurons after early neonatal hypoxia-ischemia. J. Neurosci. 23, 3308–3315.

Merrill, J.E., Scolding, N.J., 1999. Mechanisms of damage to myelin and oligodendrocytes and their relevance to disease. Neuropathol. Appl. Neurobiol. 25, 435–458.

Mori, S., Zhang, J., 2006. Principles of diffusion tensor imaging and its applications to basic neuroscience research. Neuron 51, 527–539.

Neil, J., Miller, J., Mukherjee, P., Huppi, P.S., 2002. Diffusion tensor imaging of normal and injured developing human brain—a technical review. NMR Biomed. 15, 543–552.

Noetzel, M.J., 2004. Diagnosing "undiagnosed" leukodystrophies: the role of molecular genetics. Neurology 62, 847–848.

Oka, A., Takashima, S., 1998. Expression of the ataxia-telangiectasia gene (ATM) product in human cerebellar neurons during development. Neurosci. Lett. 252, 195–198.

Paull, T.T., Lee, J.H., 2005. The Mre11/Rad50/Nbs1 complex and its role as a DNA double-strand break sensor for ATM. Cell 4.

Peters, A., 2002. The effects of normal aging on myelin and nerve fibers: a review. J. Neurocytol. 31, 581–593.

Petrini, J.H., Stracker, T.H., 2003. The cellular response to DNA double-strand breaks: defining the sensors and mediators. Trends Cell Biol. 13, 458–462.

Pierpaoli, C., Basser, P.J., 1996. Toward a quantitative assessment of diffusion anisotropy. Magn. Reson. Med. 36, 893–906.

Pierpaoli, C., Jezzard, P., Basser, P.J., Barnett, A., Di Chiro, G., 1996. Diffusion tensor MR imaging of the human brain. Radiology 201, 637–648.

Seemanova, E., Passarge, E., Beneskova, D., Houstek, J., Kasal, P., Sevcikova, M., 1985. Familial microcephaly with normal intelligence, immunodeficiency, and risk for lymphoreticular malignancies: a new autosomal recessive disorder. Am. J. Med. Genet. 20, 639–648.

Shiloh, Y., 2003. ATM and related protein kinases: safeguarding genome integrity. Nat. Rev., Cancer 3, 155–168.

Shiloh, Y., 2006. The ATM-mediated DNA-damage response: taking shape. Trends Biochem. Sci. 31, 402–410.

Stark, D., Bradley, W.G., 1992. Magnetic Resonance Imaging. Mosby.

Stoppa-Lyonnet, D., Girault, D., LeDeist, F., Aurias, A., 1992. Unusual T cell clones in a patient with Nijmegen breakage syndrome. J. Med. Genet. 29, 136–137.

Stracker, T.H., Theunissen, J.W., Morales, M., Petrini, J.H., 2004. The Mre11 complex and the metabolism of chromosome breaks: the importance of communicating and holding things together. DNA Repair (Amst.) 3, 845–854.

Sundgren, P.C., Dong, Q., Gomez-Hassan, D., Mukherji, S.K., Maly, P., Welsh, R., 2004. Diffusion tensor imaging of the brain: review of clinical applications. Neuroradiology 46, 339–350.

Taalman, R.D., Hustinx, T.W., Weemaes, C.M., Seemanova, E., Schmidt, A., Passarge, E., Scheres, J.M., 1989. Further delineation of the Nijmegen breakage syndrome. Am. J. Med. Genet. 32, 425–431.

Taylor, A.M., Byrd, P.J., 2005. Molecular pathology of ataxia telangiectasia. J. Clin. Pathol. 58, 1009–1015.

Tofts, P., 2002. Quantitative MRI of the Brain: Measuring Changes Caused by Disease. John Wiley.

Uziel, T., Lerenthal, Y., Moyal, L., Andegeko, Y., Mittelman, L., Shiloh, Y., 2003. Requirement of the MRN complex for ATM activation by DNA damage. EMBO J. 22, 5612–5621.

van der Burgt, I., Chrzanowska, K.H., Smeets, D., Weemaes, C., 1996. Nijmegen breakage syndrome. J. Med. Genet. 33, 153–156.

Varon, R., Vissinga, C., Platzer, M., Cerosaletti, K.M., Chrzanowska, K.H., Saar, K., Beckmann, G., Seemanova, E., Cooper, P.R., Nowak, N.J., Stumm, M., Weemaes, C.M., Gatti, R.A., Wilson, R.K., Digweed, M., Rosenthal, A., Sperling, K., Concannon, P., Reis, A., 1998. Nibrin, a novel DNA double-strand break repair protein, is mutated in Nijmegen breakage syndrome. Cell 93, 467–476.

Watters, D.J., 2003. Oxidative stress in ataxia telangiectasia. Redox Rep. 8, 23–29.

Weemaes, C.M., Hustinx, T.W., Scheres, J.M., van Munster, P.J., Bakkeren, J.A., Taalman, R.D., 1981. A new chromosomal instability disorder: the Nijmegen breakage syndrome. Acta Paediatr. Scand. 70, 557–564.

Weitzman, M., Carson, C.T., Scwartz, R.A., Stracker, T.H., Lilly, C.E., Lee, D.V., 2003. Using viruses to study the cellular DNA damage response.

You, Z., Chahwan, C., Bailis, J., Hunter, T., Russell, P., 2005. ATM activation and its recruitment to damaged DNA require binding to the C terminus of Nbs1. Mol. Cell. Biol. 25, 5363–5379.

Zhu, J., Petersen, S., Tessarollo, L., Nussenzweig, A., 2001. Targeted disruption of the Nijmegen breakage syndrome gene NBS1 leads to early embryonic lethality in mice. Curr. Biol. 11, 105–109.